This is a post-print of a paper published in the Environmental Geology and Health, in 2020. The paper was submitted on 11 May 2020, and this is the submitted version, as requested by the Publisher Policy.

Re: "Naturally occurring asbestos in quarries: southern Spain as a case study"

Full author list:
Andrea Bloise; andrea.bloise@unical.it
Claudia Ricchiuti; claudia.ricchiuti@hotmail.it
Rafael Navarro; r.navarro@igme.es
Rosalda Punturo; punturo@unict.it
Gabriele Lanzafame; gabriele.lanzafame@gmail.com
Dolores Pereira; mdp@usal.es

https://doi.org/10.1007/s10653-021-00811-7
Received 11 May 2020
Accepted 07 January 2021
Published 21 January 2021

Environmental Geochemistry and Health

Naturally occurring asbestos in quarries: southern Spain as a case study

--Manuscript Draft--

Manuscript Number:	
Full Title:	Naturally occurring asbestos in quarries: southern Spain as a case study
Article Type:	Original Research
Keywords:	Asbestos; NOA; Fibres; Spain
Corresponding Author:	ANDREA BLOISE Università della Calabria Rende, Italia ITALY
Corresponding Author Secondary Information:	
Corresponding Author's Institution:	Università della Calabria
Corresponding Author's Secondary Institution:	
First Author:	ANDREA BLOISE
First Author Secondary Information:	
Order of Authors:	ANDREA BLOISE
	Claudia Ricchiuti
	Rafael Navarro
	Rosalda Punturo
	Gabriele Lanzafame
	Dolores Pereira
Order of Authors Secondary Information:	
Funding Information:	
Abstract:	The Nevado-Filábride Complex (NFC) area (southern Spain) is well known for the widespread mining and quarrying activities. Serpentinite and metabasite rock types are extracted, processed and traded as building and ornamental stones. Due to possible presence of Naturally Occurring Asbestos (NOA) minerals in these lithotypes, the aim of the investigation of this paper is to discern about the presence of these fibrous minerals and to characterize them in detail. In order to do this, seven serpentinite rock samples were collected in four quarries located in Sierra Nevada and Sierra de los Filabres (South-eastern Spain) and studied by X-ray powder diffractometry (XRPD), Scanning Electron Microscopy combined with Energy-Dispersive Spectrometry (SEM/EDS), Differential scanning calorimetry (DSC), Derivative Thermogravimetry (DTG) and by X-ray Synchrotron microtomography (SR-μCT). The investigation of asbestos minerals is very important not only from a scientific point of view, but also from a legislative one, especially for the administrative agencies that have to take decisions with regards to the implementation of health protection to workers (e. g., quarry excavations, road yards, civil constructions, building stones).
Suggested Reviewers:	Alessandro Pacella Universita degli Studi di Roma La Sapienza Dipartimento di Ingegneria Civile Edile e Ambientale alessandro.pacella@uniroma1.it Expert on asbestos minerals
	Michele Mattioli Universita degli Studi di Urbino Carlo Bo michele.mattioli@uniurb.it Natural occurring asbestos (NOA) expert

Powered by Editorial Manager® and ProduXion Manager® from Aries Systems Corporation

	Robert Kusiorowski Politechnika Slaska w Gliwicach, Department of Inorganic, Analytical Chemistry and Electrochemistry, Gliwice, Poland r.kusiorowski@icimb.pl Thermal analysis expert
	Gianluca Vignaroli Universita degli Studi di Roma La Sapienza Dipartimento di Biologia e Biotecnologie Charles Darwin gianluca.vignaroli@uniroma3.it Natural occurring asbestos (NOA) expert
	Francesco Turci Universita degli Studi di Torino Dipartimento di Chimica francesco.turci@unito.it Expert in asbestos-related diseases

Powered by Editorial Manager® and ProduXion Manager® from Aries Systems Corporation

Manuscript

Click here to access/download;Manuscript;Naturally occurring asbestos Spain.docx

Click here to view linked References

Naturally occurring asbestos in quarries: southern Spain as a case study

Andrea Bloise, Claudia Ricchiuti, Rafael Navarro, Rosalda Punturo, Gabriele Lanzafame, Dolores Pereira

Andrea Bloise

Department of Biology, Ecology and Earth Sciences, University of Calabria, I-87036 Rende, CS, Italy

Claudia Ricchiuti, Rosalda Punturo, Gabriele Lanzafame

Department of Biological, Geological and Environmental Sciences, University of Catania, I-95129 Catania, Italy

Rafael Navarro, Dolores Pereira

CHARROCK Research Group. University of Salamanca, Plaza de los Caídos s/n, 37008 Salamanca, Spain

Geology Department, Science Faculty, University of Salamanca, Plaza Merced s/n, Salamanca 37008, Spain

Corresponding author:

Andrea Bloise,

Department of Biology, Ecology and Earth Sciences, University of Calabria, I-87036 Rende, CS,

Italy, Cubo 15b, 87036, tel./fax. +390984 493588,

e-mail: andrea.bloise@unical.it

orcid: https://orcid.org/0000-0003-0661-1032

Abstract

The Nevado-Filábride Complex (NFC) area (southern Spain) is well known for the widespread mining and quarrying activities. Serpentinite and metabasite rock types are extracted, processed and traded as building and ornamental stones. Due to possible presence of Naturally Occurring Asbestos (NOA) minerals in these lithotypes, the aim of the investigation of this paper is to discern about the presence of these fibrous minerals and to characterize them in detail. In order to do this, seven serpentinite rock samples were collected in four quarries located in Sierra Nevada and Sierra de los Filabres (South-eastern Spain) and studied by X-ray powder diffractometry (XRPD), Scanning Electron Microscopy combined with Energy-Dispersive Spectrometry (SEM/EDS), Differential scanning calorimetry (DSC), Derivative Thermogravimetry (DTG) and by X-ray Synchrotron microtomography (SR-μCT). The investigation of asbestos minerals is very important not only from a scientific point of view, but also from a legislative one, especially for the administrative agencies that have to take decisions with regards to the implementation of health protection to workers (e. g., quarry excavations, road yards, civil constructions, building stones).

Keywords: Quarries, Asbestos, NOA, Spain

Introduction

Ophiolite rocks are fragments of oceanic lithosphere composed of mafic and ultramafic rocks (i.e. metabasite and serpentinite), commonly known as greenstone (Punturo et al. 2018a; Pereira et al. 2005; Pereira 2012; Navarro et al. 2013) because of their typical dark greenish colour. Due to their aesthetic features and to their mechanical characteristics (i.e. high tensile strength, flexibility, high heat resistance), these rocks have been used as building and dimension stones, representing an important economic resource in many areas around the world (Pereira et al. 2007; 2013; Pereira and Peinado 2012; Punturo et al. 2018b). Therefore, greenstone rocks have been intensively mined worldwide and trade for international commerce (Kazan-Allen, 2005) since the past. Nevertheless, since ophiolite rocks represent a main source for asbestos minerals, many studies have pointed out that the substantial exploitation of greenstones could represent a risk to the human health related to the inhalation of potentially containing asbestos fibres (Belluso et al. 2020). The term “asbestos” (regulated-asbestos) refers to a group of six fibrous silicate minerals belonging to serpentine (i.e. chrysotile) and amphibole (i.e. tremolite, actinolite, anthophyllite, amosite, crocidolite) mineral groups (IARC 2012). Regarding to the dimensional definition, World Health Organization (WHO, 1997) established that fibres with length >5 μm and aspect ratio (i.e., length divided by width) ≥3:1

are fibres of respirable size. The hazard lies in the fact that, depending on their size, these fibres are able to penetrate into the lungs and consequently may trigger asbestos-related diseases (IARC 2012; Pavlisko and Sporn 2014). Epidemiological studies show that many pathology cases have been registered as developed on asbestos workers (Ross and Nolan 2003). In particular, three main disease types have been documented directly related to asbestos: i) asbestosis; ii) lung cancer; and iii) mesothelioma. Furthermore, an association between the increase in the onset of lung diseases and the non-occupational exposure to asbestos fibres has been also observed, showing that they represent a risk for both workers and people who live near to Naturally Occurring Asbestos (NOA) outcrops (Acosta et al. 1997; Constantopoulos 2008; Pereira et al. 2008; Pugnaloni et al. 2013; Bloise et al. 2014; Berk et al. 2014; Baumann et al. 2015; Bellomo et al. 2018; Cagnard and Lahondère 2020). The term NOA refers to both regulated and non-regulated fibrous minerals present in rocks (i.e., serpentinite or altered ultramafic rocks) and soils, that have not been extracted for commercial purposes (Harper 2008). Activities related to stone processing (e.g., road construction, excavation) as well as weathering processes (e.g., erosion) may disturb NOA bearing rocks (e.g., Vignaroli et al. 2014; Gaggero et al. 2017; Pierdzig 2019; Bloise and Miriello 2018; Bloise et al. 2012; 2016a; 2017a; 2019a) causing the release of potentially inhalable fibres in the environment. It has been noted by the scientific community that minerals with fibrous habit, even if not belonging to the asbestos category such as erionite, ferrierite, antigorite, todorokite and others alike may also have toxic effects on human health (Bloise et al. 2020a; Ballirano et al. 2018 a, b; Gualtieri et al. 2018). In Spain, owing to possible health problems asbestos correlate, the rock-processing in quarries sitting on greenstone lithotypes is regulated by the Spanish law (Real Decreto, 396/2006), as there is evidence of the harmful effects of these fibres on people employed at these activities. The awareness on risk related to asbestos exposure leads to a considerable interest on the identification of regulated and non-regulated mineral fibres in rocks. In order to point out the eventual presence of asbestos minerals within serpentinite, this study focuses on a comprehensive mineralogical characterization of seven serpentinite rock samples collected from quarries located in Sierra Nevada and Sierra de los Filabres areas (Southeastern Spain) (Navarro et al. 2018). These serpentinite rocks have been used in a large number of applications such as ornamental stones, aggregates and inert material (Pereira et al. 2013; Navarro et al. 2018). In this scenario, the present paper provides detailed information related to the distribution of NOA in the NFC area, with the aim of improving the territory mapping and to reduce the environmental asbestos exposure.

Geological setting

The studied samples were collected at several quarries from Sierra Nevada and Sierra de los Filabres (Southeastern Spain). In particular, these quarries are located in the Nevado-Filabride Complex (NFC) (Fig. 1), an allochthonous metamorphic complex placed in the lowest position of the Internal Zones of the Betic Cordillera (Martin-Algarra et al. 2004). This complex can be subdivided into two tectonic units: the lower unit (or Veleta Unit) and the upper unit (or Mulhacen Unit). According to Sanz de Galdeano and López-Garrido (2016), both units share the same sequence from bottom to top: dark schist with interbedded quartzites (Carboniferous), quartzites, mica schist with garnets (Permian), and interbedded quartzites, schist and marble (Permian-Triassic). Interlayed within the sequence, metamorphosed igneous rocks, principally metabasite and tourmaline-bearing orthogneisse are common. Metabasite rocks, whose thickness ranges from several centimeters to hundreds meters, occur within the mica schist and marble units, with the exception of the "Barranco de San Juan" outcrop, which is placed in the dark schist unit. According to Sanz de Galdeano and López-Garrido (2016), the metabasite rocks correspond to former basic volcanic extrusions interlayered in metasediments. Metadolerite dikes can be found as lenticular bodies of decimetric thickness partially rodingitizated, and transformed into metarodingites or eclogites during metamorphism (Puga et al. 2011).

Sampling

Samples were collected as follows: two of them in Sierra Nevada: "Barranco de San Juan" (samples VG1 and VG2) and "Nigüelas" (sample NG) and the other four ones in Sierra de los Filabres: "Virgen del Rosario" (samples VM1 and VM2) and "La Carrasca" (samples CA1 and CA2) (Fig. 1). The quarry "Barranco de San Juan" is located in Güejar Sierra (Granada). It is the oldest serpentinite quarry for dimension stone in Spain. The quarrying activity began in the 16th century and it was close in the middle of the 20th century. The commercial variety was known as "Verde Granada". There are many monuments all over the country where this stone was employed, such as the Monastery of El Escorial (16th century) and the Royal Palace (18th century) in Madrid and the Palace of Carlos V (16th century) and the Royal Chancellery (16th century) in Granada (Navarro et al., 2015). The present interest in this quarry is due to its importance as potential source of material for restoration of monuments and historical buildings. The quarry "Nigüelas" is located in Nigüelas (Granada); it is a small quarry opened in the seventies of the 20th century; it was planned for extracting dimension stone but, subsequently, it had to be closed by owners because of the high asbestos content. The quarry "Virgen del Rosario" is located in Macael (Almería); it is a still active quarry for extraction of white,

grey and yellow marble that is marketed as "Verde Macael" and it had been used both in national and international buildings; some significant examples can be observed in the Almudena Cathedral (20th century) in Madrid and in many civil buildings across Spain. Finally, the quarry "La Carrasca" is located in Albanchez (Almería) and the extracted serpentinite is marketed as dimension stone. Depending on the demand, the quarry has a discontinuous exploiting activity and, unlike the other mentioned serpentinite rocks, the marketed serpentinite does not have any commercial name. In the specific case of this work, the samples studied are serpentinite rocks showing high degree of carbonation (Navarro et al. 2018), such that many varieties of these rocks are included in the technical datasheet of marbles even though their mineralogical, geochemical, physical and mechanical properties are different respect to marbles (Navarro et a. 2018).

Analytical methods

The seven serpentinite rock samples have been studied by means of several laboratory techniques such as X-ray powder diffraction (XRPD), scanning electron microscopy SEM equipped with an energy-dispersive X-ray spectrometer (EDS), Differential scanning calorimetry (DSC), Derivative Thermogravimetry (DTG) and X-ray Synchrotron microtomography (SR-μCT). Thermal analysis has been very useful either for the identification of the serpentine group (i.e. chrysotile, lizardite, antigorite, and polygonal serpentine) and for the characterization of amphibole asbestos (Bloise et al. 2017b). The XRPD analysis was performed by using the Rigaku SmartLab (Rigaku Europe SE, Germany) diffractometer, equipped with CuKa radiation and SC-70 detector at 40 kV and 100 mA. Scans were collected in the range of 6°-75° 2θ with a step interval of 0.01° and step counting time of 2 s. SmarlLab Studio II software was used to identify the mineral phases in each X-ray powder spectrum, experimental peaks being compared with ICDD (PDF2.DAT) reference patterns. DSC/DTG analyses were performed with a Netzsch STA 449 C Jupiter (Netzsch-Gerätebau, Germany) in the temperature range 30-1200°C with a heating rate of 10°C·min^{-1}, and under air flow of 30 mL·min^{-1}. Instrumental precision has been verified by five repeated collections on a kaolinite reference sample, revealing acceptable reproducibility (instrumental theoretical T precision of ± 1.2°C), DSC detection limit < 1 μW. Netzsch proteus thermal analysis software (Netzsch-Gerätebau, Germany) was used to identify exo-thermic, endo-thermic and derivative thermogravimetry (DTG) peaks. For SEM analysis, a fragment of each specimen was coated with graphite after being fixed on SEM stub using double-sided conductive adhesive tape. The specimens were examined by using Tescan-Vega\\LMU scanning electron microscope, equipped with an energy-dispersive X-ray spectrometer (EDS) Edax Neptune XM4 60, operating at 15 kV accelerating voltage and 20 nA beam

current conditions. The 3D study of the samples was carried out by using Synchrotron Radiation X-ray computed microtomography (SR-μCT) in phase-contrast mode (Cloetens et al. 1997) at the SYRMEP beamline of the Elettra synchrotron laboratory (Basovizza, Italy). Samples were cut parallelepiped shaped with size of about 4 × 4 × 20 mm. Experiments were performed in white beam configuration (Baker et al., 2012), employing a filtered (1 mm Si + 1 mm Al) polychromatic X-ray beam delivered by a bending magnet source in transmission geometry. For each experiment 1800 projections were acquired over a total scan angle of 180° with an exposure time/projection of 2 s and sample-to-detector distance fixed at 150 mm. The employed detector was a 16 bit, air-cooled, sCMOS camera (Hamamatsu C1144022C) with a 2048 × 2048 pixels chip. The effective pixel size of the detector was set at 1.95 × 1.95 μm^2, yielding a maximum field of view of ca. 4 mm^2. Microtomographic scans were acquired in local region of interest mode (Maire and Withers 2014). The reconstruction of the 2D tomographic slices was done with the Syrmep Tomo Project (STP) house software suite (Brun et al. 2017). A single-distance phase-retrieval algorithm (Paganin et al. 2002) combined with Filtered Back-projection algorithm (Herman 1980) was employed to the sample projections to improve the consistency of the quantitative analysis. The reconstructed volumes were investigated in order to evaluate the veins/void of the samples. The 3D image treatment and analysis were performed by means of Fiji software (Schindelin et al. 2012) using the procedure described by Bloise et al. (2020b). The original stacks of slices were first cropped for extracting, for each sample, the Volumes of Interest (VOIs). In order to retrieve the veins/voids phase, VOIs were segmented by manual thresholding. This procedure allowed to obtain binary (black and white) 3D images of the phase of interest that were analysed for retrieving the porosity values, calculated as volume of pores/total volume. The 3D renderings of the VOIs were obtained by means of VGStudio Max 2.2 software.

Results

Mesoscale features of serpentinite rocks

Based on the mesoscopic observations, a high variability of serpentinite coming from different outcrops is notable (Fig.s 2, 3), mainly due to the complex origin of these rocks (Navarro et al. 2018). Figure 2 shows a view of the quarries and figure 3 shows a close detail of the outcrops where the samples come from. The samples show various microstructural features: i) massive, ii) with evident presence of veins, and iii) totally fibrous (Fig. 3). Moreover, depending on the carbonation degree, some samples show various green colour tonality. Both samples from the quarry “Barranco de San

Juan" (VG1 and VG2) are massive and show dark and light green colour, respectively; differently, sample NG from the quarry "Nigüelas" appears totally fibrous. Samples from quarry "Virgen de Rosario" show massive structure (VM1) and evident veins (VM2). Rock collected from the quarry "La Carrasca" are very different from each other; indeed, CA1 is fibrous and CA2 is massive.

XRPD characterization

XRPD patterns show that the investigated specimens are composed of serpentine minerals, amphiboles, dolomite, calcite, followed by chlorite, magnetite, quartz and clay minerals, which were detected less frequently and at low amount (Table 1). Since XRPD was not able to distinguish among the different serpentine minerals, a further characterization of each sample was performed by thermal analysis (DSC/DTG).

DSC/DTG characterization

The data of the thermal analysis reduce the ambiguities in the identification of the serpentine polymorphs. The correspondence between the endothermic and exothermic effects in the DSC curves and minerals is in accordance with the literature data (Földvári 2011; Bloise et al. 2016b; 2017b; 2019b). In the same way, the maximum peak loss rate recorded on DTG curves was in accordance with the literature data (Bloise et al. 2017b; 2016b; 2019b). Regarding asbestos minerals, the endothermic peaks in a temperature range of 605–650 °C (Fig.s 3, 4) were linked to chrysotile breakdown whereas amphiboles showed endothermic peaks in the range 1039-1070 °C (Fig.s 4, 5). Samples NG, VM1 and CA2 were the only one in which chrysotile was not identified. Other serpentine polymorphs such as lizardite (samples VG1, VG2 and CA2) and antigorite (samples VG2, NG, VM2 and CA2) were also detected. Polygonal serpentine was only detected in three samples (VG1, NG, CA2). Magnetite, chlorite, calcite, dolomite and quartz were also identified at variable amounts in some samples (Table 2). The exothermic peaks at about 850 °C and 1100 °C (Table 2) were interpreted as the crystallization of forsterite and pyroxene deriving from serpentine and amphiboles breakdown (Bloise et al. 2017b).

SEM/EDS investigation

The observation of SEM images allowed detailed investigation on the fibres morphology, to determine their size and to compare them with regulated asbestos size (WHO 1997). Results highlighted the presence of serpentine and amphibole in all of the samples occurring either with

fibrous and non-fibrous habit. Chrysotile was observed, with the typical appearance as bundles of separable fibres (Fig. 6a-c) or as fibres that, in turn, are composed of fibrils with smaller diameter and tend to split up along their elongation axis (Fig. 6b; sample CA1). Regarding amphiboles, samples show the presence of tremolite that occurs either as prismatic single crystals and with fibrous habit (Fig. 6 a-d) with small diameter and length exceeding 5 μm (i.e. asbestos classified). Sample NG showed fibrous appearance already observed at the mesoscale, which can be explained by the presence of tremolite (Fig. 7a), since chrysotile has not been detected. By paying special attention to morphology, it is possible to observe the occurrence of very long and thin fibres with the tendency to split into thinner ones because of their good flexibility (asbestiform tremolite; Fig.s 7b, c, d); these fibres occur in addition to long and thin crystals exhibiting prismatic shape, but lacking any flexibility (non-asbestiform tremolite. Fig.s 7a, 7d). Because of their size, prismatic crystals may be often mistaken for bundles of fibrils. Similarly, cleavage fragments, which are the results of breakage along preferred planes of cleavage of larger crystals, may look like bundles of fibrils. Since these particles are so small that can be inhaled, several investigation methodologies are nowadays dedicated to the study of non-asbestos minerals toxicity (Belluso et al. 2017). The morphology of chrysotile asbestos particles is different compared to the amphibole asbestos; the former usually consists of fibrils that arise either singly or as bundles, while amphibole consists of fibres mostly with parallel-sides (Fig.s 6, 7). Table 3 shows the chemical composition (oxide and atom per formula unit) of chrysotile fibres in samples VG1, VG2, VM2 and CA1. The data revealed a quite similar chemical composition, with SiO_2 values ranging from 42.14 to 47.34 wt.% and MgO ranging from 42.12 to 46.85 wt.%. Al_2O_3 content varies from a minimum of 2.46 wt.% to a maximum of 4.97 wt%. FeO was always found in chrysotile samples (Table 3) in variable concentration, ranging between 2.67 and 7.36 wt. % with an average of 4.73 wt.%. According to the cation distribution model known to date (Stroink et al. 1980; Hardy and Aust 1995), Al^{3+} may substitute both Si^{4+} and Mg^{2+} in the tetrahedral and octahedral sheets respectively, and both Fe^{2+} and Fe^{3+} ions can replace Mg^{2+} in the octahedral sheet, although in limited amount (Ballirano et al. 2017). In three out of four samples, a low amount of Cr was detected (about 0.29 wt.%) although not in all analysis points (Table 3). A similar trend was detected for Ni, which was detected in all samples, but inconsistently (Table 3), with an average of 1.68 wt.%. The use of the energy dispersive spectrometry (EDS) spot analysis was crucial for the identification of amphibole asbestos. Chemical analysis of amphiboles were plotted on the binary Si vs $Mg/(Mg + Fe^{2+})$ diagram, which is a standard presentation for classification of the calcic amphiboles (Leake et al. 1997; Hawthorne and Oberti 2007). Amphibole compositions plot in the field of tremolite, tremolite-hornblende, actinolite-hornblende, fibrous magnesio-hornblende and tschermakite (Fig. 8). However, only analyses of samples CA1 and NG plot in the tremolite domain. The semi-quantitative

chemical composition of several tremolite fibres as determined by SEM/EDS analyses are reported in Table 4. The chemical composition of the tremolite is consistent with the elements present in the its stoichiometric composition (Si, Mg, Ca). Regarding ferrous iron content in tremolite in sample CA1, it ranges from a minimum of 1.63 wt% to a maximum of 4.98 wt% with average value of 3.34 wt% while in the tremolite detected in the sample NG, the amount of Fe ranges from 1.52 wt% to 4.24 wt% with an average value of 2.34 wt.%. From the chemical point of view, the average amount of iron detected in tremolite of the NFC quarries is in agreement with the iron content of other samples of tremolite worldwide (e.g., Pacella et al. 2010). Moreover, in one sample (CA1) low amounts of Cr was also detected.

SR-μCT investigation and three-dimensional image analysis

Lately, synchrotron radiation X-ray computed microtomography (SR-μCT) has become a widely used non-destructive technique for unravelling complex rock textures, since it allows to obtain a real representation of the three-dimensional (3D) inner structure of the samples with micrometric to nanometric spatial resolution, preserving at the same time the specimens for further studies. Indeed, the possibility to investigate 3D images allows a precise and reliable quantitative analysis of the amount and morphology of rock components such as crystals and pores (Baker et al. 2012; Lanzafame et al. 2020) or textures such as veins and fibres (Militello et al. 2019; Punturo et al. 2019; Bloise et al. 2020b). DSC/DTG and SEM results were consistent with SR-μCT data. In fact, following the work of Bloise et al. (2020b), as can be seen in figures 9a and 9b (sample CA1) in the samples in which veins and/or voids were present the development of fibrous phases of chrysotile and fibrous amphibole was identified. Inspection on the 2D slices of the veins obtained by SR-μCT, show that in some section of the sample there are portions in which the fibres were evident because not grown in the same direction. In the veins, the asbestos fibers (chrysotile and tremolite) crystallize as bundles of fibers, while in other parts of the sample the veins are filled with non-fibrous phases since there are no voids. The investigation of 3D reconstructions also reveals the interweaving of the veins/voids within the serpentinite matrix. On the other hand, in samples with no veins (Fig. 9c, d), the growth of fibrous phases was prevented (Table 1, sample CA2). Lamellar phases such as antigorite and lizardite are predominantly found in the sample CA2, whereas fibrous phases are absent. Small magnetite crystals visible as bright dots were also identified (Fig. 9 c, d).

Discussion

The main mineralogical characteristics of the studied serpentinite samples are similar to those ones found in other similar lithotypes from quarries worldwide (e.g., Belluso et al. 2020; Pacella et al.

2010; Punturo et al. 2019), in which a prevalence of chrysotile and asbestos tremolite has been observed. Despite the fibrous morphology detected at the scale of the outcrop, not every fibre fit the properties (i.e., respirable size, chemical, flexibility) of asbestos (Gualtieri 2017). However, the integration of various analytical techniques (XRPD, EDS/SEM, DSG/DTG and SR-μCT) constrains the mineralogical, chemical and morphological properties, of lamellar and fibrous phases, certifying that fibrous mineral can truly be classified as asbestos. As for the fibrous but non-asbestos classified, polygonal serpentine and magnesio-hornblende were also detected. Among the minerals considered as asbestos, chrysotile and tremolite, have been identified. The component that decisively affects fibres toxicity depends on combining factors including the size of the inhaled fibres as well as the content of toxic elements (Turci et al. 2017). Many research works highlighted that length is a key factor in the pathogenicity of mineral asbestos. In particular, fibres longer than 5 μm in length are associated with the onset of asbestos related lung disease (Mossman and Pugnaloni 2017). Most of the chrysotile and tremolite fibres studied in this work, showed lengths that are in accordance with this criterion. Moreover, chrysotile and tremolite asbestos contain potentially toxic elements, specifically Fe, Cr, and Ni as minor elements in their crystalline structure posing therefore human health at risk. It has been demonstrated that asbestos toxicity is related to the presence of metals (i.e., Fe, Ni, Cr) as a catalyst of the Fenton reaction leading to the generation of free radicals and reactive oxygen species (ROS) (Turci et al. 2017). The finding of relatively high concentrations of such metals in the samples of chrysotile and tremolite asbestos in the studied samples is in agreement with the literature data, which show that in these two types of asbestos, the detected metals (Fe, Cr, Ni) are often present in concentration up than 1000 ppm (Bloise et al. 2016c). It must also be considered that, these toxic elements can be mobilized and spread into various terrestrial environments and penetrate in the human body. Indeed, due to its co-occurrence with toxic metals, asbestos has been reported to introduce metals in soil, water and air systems triggering a danger to human health (Gwenzi 2019; Mistikawy et al. 2020). Another aspect to consider is that, both types of fibres, when released, can travel along considerable distance due to their aerodynamic features (Kohyama 1989). The long distances suggest the possibility of non-occupational human exposure and health risks occurring further away from the original quarries source. However, if these rocks are not disturbed by human actions (e.g. road construction, excavation) it is highly improbable that the fibres are airborne and therefore dangerous for human health. On the other hand, it has to be taken into account that rocks can be disturbed by natural events such as natural weathering processes, earthquakes and human-related disasters (Perkins et al. 2007; Kashimura et al. 2015). In this perspective, the voluntary closure of Nigüelas quarry by its owners is a model example of synergy between the assessment of the risk of asbestos by scientists and people concerned about the health of the workers. In our opinion, the

monuments or artefacts built with the rocks extracted from the quarries of Barranco de San Juan, Nigüelas, Virgen del Rosario and La Carrasca , do not have the possibility of releasing fibres into the environment due to the following reasons: i) they are usually sprinkled with protective resins; ii) they are usually products that are not subject to weathering, because they are inside buildings (i. e., altar of churches, columns and holy water fonts) (e.g., Navarro et al. 2015; 2018). However, it is good practice to monitor the state of conservation of monuments and artefacts built on these materials and, if eventually deteriorated, to carry out restoration, since fractures are often filled with these fibrous minerals, can act as weakness surfaces, and cause the breakdown of the pieces, with unexpected consequences (Yoon et al. 2020; Erskine 2020; Navarro et al. 2018).

Conclusions

In this study, seven serpentinite rocks have been investigated in order to assess the presence of naturally occurring asbestos. XRPD, DSC/DTG, SEM/EDS, and SR-µCT methods have been successfully applied for the determination of asbestos hosted in complex serpentinite multi-phase samples. The identified asbestos minerals are tremolite and chrysotile. The results obtained by comparing data indicate that five out of seven samples contain potentially harmful fibres, tremolite is present in only two samples (CA1 and NG), whereas chrysotile has been found in four samples (CA1, VM2, VG2, VG1). This study evidences an asbestos contamination of the following quarries: Barranco de San Juan (Granada) and Nigüelas (Granada). On the other hand, the quarries of Virgen del Rosario and La Carrasca were partially contaminated by asbestos since two studied samples (VM1 and CA2) do not contain any asbestos. Although sample CA1 (La Carrasca-quarry) could be considered the most harmful to human health due to the concomitant presence of chrysotile and tremolite asbestos. Such differences observed in the same quarry (e.g., La Carrasca) can be related to the different geochemical/petrological processes involved in the formation of asbestos. This suggest that workers should take caution during the phases of extraction of the rocks in the quarries. In this regard, any further extension of the quarries requires detailed mineralogical studies, aimed at reducing the possibility of intercepting asbestos minerals. In conclusions, the results of this study are strategic as could be used to define a sampling plan for identifying the areas around the quarries polluted with asbestos. Besides, the results of our study have general implications regarding the use of consolidated experimental techniques for the determination of asbestos minerals in rocks.

Acknowledgments: We thank Lucia Mancini, responsible of the SYRMEP beamline of ELETTRA Synchrotron laboratory (Trieste, Italy). The University of Salamanca is acknowledged for the USAL Research Funding to support the members of the GIR CHARROCK.

Declarations

Funding

No funding was received.

Conflicts of interest

The authors declare that that there is no conflict of interest

Availability of data and material

All the raw data and material used for this research is available at the University of Calabria and University of Catania for request.

References

Acosta, A., Pereira, M.D., Shaw, D.M., & Bea, F. (1997). Serpentinización de la peridotita de Ronda (cordillera Betica) comorespuesta a la interacción con fluidos ricos en volátiles: comportamiento del boro. *Revista de la Sociedad Geológica de España*, 10, 99- 106.

Baker, D.R., Mancini, L., Polacci, M., Higgins, M.D., Gualda, G.A.R., Hill, R.J., et al. (2012). An introduction to the application of X-ray microtomography to the three-dimensional study of igneous rocks. *Lithos*, 148, 262–276.

Ballirano, P., Bloise, A., Gualtieri, A.F., Lezzerini, M., Pacella, A., Perchiazzi, N., et al. (2017). The Crystal Structure of Mineral Fibers. In A.F. Gualtieri (Ed.), *Mineral Fibers: Crystalchemistry, Chemical-Physical Properties, Biological Interaction and Toxicity* (pp. 17-53). London, UK: Mineralogical Society of Great Britain and Ireland.

Ballirano, P., Pacella, A., Bloise, A., Giordani, M., & Mattioli, M. (2018a). Thermal Stability of Woolly Erionite-K and Considerations about the Heat-Induced Behaviour of the Erionite Group. *Minerals*, 8, 28.

Ballirano, P., Bloise, A., Cremisini, C., Nardi, E., Montereali, M.R., & Pacella, A. (2018b). Thermally induced behavior of the K-exchanged erionite: a further step in understanding the structural modifications of the erionite group upon heating. *Periodico di Mineralogia*, 87, 123-134.

Baumann, F., Buck, B.J., Metcalf, R.V., McLaurin, B.T., Merkler, D.J., & Carbone, M. (2015). The presence of asbestos in the natural environment is likely related to mesothelioma in young individuals and women from Southern Nevada. *Journal of Thoracic Oncology,* 10 (5), 731-737.

Bellomo, D., Gargano, C., Guercio, A., Punturo, R., & Rimoldi, B. (2018). Workers' risks in asbestos contaminated natural sites. *Journal of Mediterranean Earth Science, 10,* 97–106.

Belluso, E., Cavallo, A., & Halterman, D. (2017). Crystal habit of mineral fibres. In A.F. Gualtieri (Ed.), *Mineral Fibers: Crystal Chemistry, Chemical-Physical Properties, Biological Interaction and Toxicity* (pp. 65-109). London, UK: European Mineralogical Union.

Belluso, E., Baronnet, A., & Capella, S. (2020). Naturally Occurring Asbestiform Minerals in Italian Western Alps and in Other Italian Sites. *Environmental & Engineering Geoscience*, *26*(1), 39-46.

Berk, S., Yalcin, H., Dogan, O. T., Epozturk, K., Akkurt, I., & Seyfikli, Z. (2014). The assessment of the malignant mesothelioma cases and environmental asbestos exposure in Sivas province, Turkey. *Environmental geochemistry and health*, *36*(1), 55-64.

Bloise, A., Belluso, E., Critelli, T., Catalano, M., Apollaro, C., Miriello, D., & Barrese, E. (2012). Amphibole asbestos and other fibrous minerals in the meta-basalt of the Gimigliano-Mount Reventino Unit (Calabria, south-Italy). *Rendiconti Online della Società Geologica Italiana*, 21, 847–848.

Bloise, A., Critelli, T., Catalano, M., Apollaro, C., Miriello, D., Croce, A., et al. (2014). Asbestos and other fibrous minerals contained in the serpentinites of the Gimigliano-Mount Reventino Unit (Calabria, S-Italy). *Environmental Earth Sciences*, 71(8), 3773-3786.

Bloise, A., Punturo, R., Catalano, M., Miriello, D., & Cirrincione, R. (2016a). Naturally occurring asbestos (NOA) in rock and soil and relation with human activities: The monitoring example of selected sites in Calabria (southern Italy). *Italian Journal of Geosciences*, 135, 268–279.

Bloise, A., Catalano, M., Barrese, E., Gualtieri, A.F., Gandolfi, N.B., Capella, S., et al. (2016b). TG/DSC study of the thermal behaviour of hazardous mineral fibres. *Journal of Thermal Analysis and Calorimetry*, 123, 2225–2239.

Bloise, A., Barca, D., Gualtieri, A.F., Pollastri, S., & Belluso, E. (2016c). Trace elements in hazardous mineral fibres. *Environmental Pollution*, 216, 314–323.

Bloise, A., Catalano, M., Critelli, T., Apollaro, C., & Miriello, D. (2017a). Naturally occurring asbestos: Potential for human exposure, San Severino Lucano (Basilicata, Southern Italy). *Environmental Earth Sciences*, 76, 648-660.

Bloise, A., Kusiorowski, R., Lassinantti Gualtieri, M., & Gualtieri, A.F. (2017b). Thermal behaviour of mineral fibers. In A.F. Gualtieri (Ed.), *Mineral Fibers: Crystalchemistry, Chemical-Physical Properties, Biological Interaction and Toxicity* (pp. 215-252). London, UK: Mineralogical Society of Great Britain and Ireland.

Bloise, A., & Miriello, D. (2018). Multi-analytical approach for identifying asbestos minerals in situ. *Geosciences*, 8(4), 133.

Bloise, A., Ricchiuti, C., Giorno, E., Fuoco, I., Zumpano, P., Miriello, D., et al. (2019a). Assessment of naturally occurring asbestos in the area of Episcopia (Lucania, Southern Italy). *Fibers*, 7(5), 45.

Bloise, A. (2019b). Thermal behaviour of actinolite asbestos. *Journal of Materials Science*, 54(18), 11784-11795.

Bloise, A., Miriello, D., De Rosa, R., Vespasiano, G., Fuoco, I., De Luca, R., et al. (2020a). Mineralogical and Geochemical Characterization of Asbestiform Todorokite, Birnessite, and Ranciéite, and Their host Mn-Rich Deposits from Serra D'Aiello (Southern Italy). *Fibers*, 8(2), 9.

Bloise, A., Ricchiuti, C., Lanzafame, G., & Punturo, R., (2020b). X-ray synchrotron microtomography: a new technique for characterizing chrysotile asbestos. *Science of the Total Environment*, 703, 135675.

Brun, F., Massimi, L., Fratini, M., Dreossi, D., Billé, F., Accardo, A., et al. (2017). SYRMEP tomo project: a graphical user interface for customizing CT recon-struction workflows. *Advanced Structural and Chemical Imaging*, 3(1), 4.

Cagnard, F., & Lahondère, D. (2020). Naturally Occurring Asbestos in France: Geological Mapping, Mineral Characterization, and Technical Developments. *Environmental & Engineering Geoscience*, *26*(1), 53-59.

Cloetens, P., Pateyron-Salome, M., Buffière, J.Y., Peix, G., Baruchel, J., Peyrin, F., et al. (1997). Observation of microstructure and damage in materials by phase sensitive radiography and tomography. *Journal of Applied Physics*, 81, 5878. https://doi.org/10.1063/1.364374.

Constantopoulos, S.H., (2008). Environmental mesothelioma associated with tremolite asbestos: Lessons from the experiences of turkey, greece, corsica, new caledonia and cyprus. *Regulatory Toxicology and Pharmacology*, 52, S110-S115.

Erskine, B. G. (2020). Geologic Investigations for Compliance with the CARB Asbestos ATCM. *Environmental & Engineering Geoscience*, *26*(1), 99-106.

Földvári, M. (2011). Handbook of thermogravimetric system of minerals and its use in geological practice. In T. Fancsik (Ed.), *Occasional papers of the Geological Institute of Hungary*. Budapest: Geological Institute of Hungary.

Gaggero, L., Sanguineti, E., Yus González, A., Militello, G.M., Scuderi, A., & Parisi, G., (2017). Airborne asbestos fibres monitoring in tunnel excavation. *Journal of Environmental Management*, 196, 583-593.

Gualtieri, A.F. (2017). Introduction. In A.F. Gualtieri (Ed.), *Mineral Fibers: Crystalchemistry, Chemical-Physical Properties, Biological Interaction and Toxicity* (pp. 1-15). London, UK: Mineralogical Society of Great Britain and Ireland.

Gualtieri, A. F. (2018). Towards a quantitative model to predict the toxicity/pathogenicity potential of mineral fibers. *Toxicology and applied pharmacology*, 361, 89-98.

Gualtieri, A., Gandolfi, N.B., Passaglia, E., Pollastri, S., Mattioli, M., Giordani, M., Ottaviani, M.F., Cangiotti, M., Bloise, A., Barca D., Vigliaturo, R., Viani, A., Pasquali, L., Gualtieri M. L. (2018). Is fibrous ferrierite a potential health hazard? Characterization and comparison with fibrous erionite. *American Mineralogist: Journal of Earth and Planetary Materials*, 103, 1044-1055.

Gwenzi, W. (2019). Occurrence, behaviour, and human exposure pathways and health risks of toxic geogenic contaminants in serpentinitic ultramafic geological environments (SUGEs): A medical geology perspective. *Science of The Total Environment*, 134622.

Hardy, J.A., & Aust, A.E. (1995). Iron in asbestos chemistry and carcinogenicity. *Chemical Reviews*, 95, 97-118.

Harper, M. (2008). 10th Anniversary critical review: naturally occurring asbestos. *Journal of Environmental Monitoring*, 10, 1394-1408.

Hawthorne, F.C., Oberti, R., Della Ventura, G., & Mottana, A. (2007). Amphiboles: Crystal chemistry, occurrence, and health issues. In F.C. Hawthorne, R. Oberti, G. Della Ventura, A. Mottana (Ed.), *Reviews in Mineralogy and Geochemistry*, (p. 545). Chantilly, VA: Mineralogical Society of America and Geochemical Society.

Herman, G.T. (1980). *Fundamentals of Computerized Tomography. Image Reconstruction from Projections.* London: Springer-Verlag.

IARC Working Group on the Evaluation of Carcinogenic Risk to Humans, (2012). IARC Monographs on the Evaluation of Carcinogenic Risks to Humans, No. 100C. Lyon: International Agency for Research on Cancer.

Kashimura, K., Yamaguchi, T., Sato, M., Yoneda, S., Kishima, T., Horikoshi, S., et al. (2015). Rapid transformation of asbestos into harmless waste by a microwave rotary furnace: application of microwave heating to rubble processing of the 2011 Tohoku earthquake. *Journal of Hazardous, Toxic & Radioactive Waste*, 19, 04014041-04014048.

Kazan-Allen, L, (2005). Asbestos and mesothelioma: Worldwide trends. *Lung Cancer*, 49S1, S3-S8.

Kohyama, N., (1989). Airborne asbestos levels in non-occupational environments in Japan. *IARC Scientific Publication*, 90, 262–276.

Lanzafame, G., Casetta, F., Giacomoni, P.P., Donato, S., Mancini, l., Coltorti, M., et al. (2020). The Skaros effusive sequence at Santorini (Greece): Petrological and geochemical constraints on an interplinian cycle. Lithos, 362-363, 105504. https://doi.org/10.1016/j.lithos.2020.105504.

Leake, B.E., Wolley, A., Arps, C.E.S., Birch, W., Gilbert, C.M., Grice, J.D., et al. (1997). Nomenclature of amphiboles: report of the subcommittee on amphiboles of the international mineralogical association, commission on new minerals and mineral names. *The Canadian Mineralogist*, 35, 219-246.

Maire, E., & Withers, P.J. (2014). Quantitative X-ray tomography. *International Materials Reviews*, 59, 1–43.

Martín-Algarra, A.C., Alonso-Chaves, F.M., Andreo, B., Azañón, J.M., Balanyá, J.C., Booth-Rea, G., et al. (2004). Zonas Internas Béticas. In J.A. Vera (Ed.), *Geología de España* (pp. 395-444). Madrid, Spain: Sociedad Geológica de España (S.G.E.)-Instituto Geológico y Minero de España (I.G.M.E.).

Militello, G.M., Bloise, A., Gaggero, L., Lanzafame, G., & Punturo, R. (2019). Multi-analytical approach for asbestos minerals and their non-asbestiform analogues: inferences from host rock textural constraints. *Fibers*, 7, 42. https://doi.org/10.3390/fib7050042

Mistikawy, J. A., Mackowiak, T. J., Butler, M. J., Mischenko, I. C., Cernak, R. S., & Richardson, J. B. (2020). Chromium, manganese, nickel, and cobalt mobility and bioavailability from mafic-to-ultramafic mine spoil weathering in western Massachusetts, USA. *Environmental Geochemistry and Health*, 1-17.

Mossman, B.T., & Pugnaloni, A. (2017). In vitro biological activity and mechanisms of lung and pleural cancers induced by mineral fibres. In A.F. Gualtieri (Ed.), *Mineral Fibers: Crystal Chemistry, Chemical-Physical Properties, Biological Interaction and Toxicity* (pp. 261–306). London, UK: European Mineralogical Union.

Navarro, R., Pereira, M.D., Gimeno, A., & Del Barrio, S. (2013). Verde Macael: a serpentinite wrongly referred to as a marble. *Geosciences*, 3, 102-113. https://doi.org/10.3390/geosciences3010102

Navarro, R., Pereira, D., Rodríguez-Navarro, C., & Sebastian-Pardo, E. (2015). The Sierra Nevada serpentinites: the serpentinites most used in Spanish heritage buildings. In D. Pereira, B. Marker, S. Kramar, B. Cooper, B. Schouenborg (Ed.), *Global Heritage Stone: Towards International Recognition of Building and Ornamental Stones* (v. 407 pp. 101-108). London (UK): Geological Society. http://dx.doi.org/10.1144/SP407.7.

Navarro, R., Pereira, D., Gimeno, A., & Del Barrio, S. (2018). Influence of natural carbonation process in serpentinites used as construction and building materials. *Construction and Building Materials*, 170, 537-546. https://doi.org/10.1016/j.conbuildmat.2018.03.100.

Pacella, A., Andreozzi G.B., & Fournier, J. (2010). Detailed Crystal Chemistry and Iron Topochemistry of Asbestos Occurring in its Natural Setting: A First Step to Understanding its Chemical Reactivity. *Chemical Geology*, 277(3-4), 197-206.

Paganin, D., Mayo, S.C., Gureyev, T.E., Miller, P.R., & Wilkins, S.W. (2002). Simultaneous phase and amplitude extraction from a single defocused image of a homogeneous object. *Journal of Microscopy*, 206, 33–40.

Pavlisko, E.N., & Sporn, T.A. (2014). Mesothelioma. In T.D. Oury, T.A. Sporn, V.L. Roggli (Ed.), *Pathology of Asbestos-Associated Disease* (pp.81-140). Berlin, Heidelberg: Springer-Verlag.

Pereira, M.D., Blanco, J.A., Yenes, M., & Peinado, M. (2005). Las serpentinitas y su correcta utilización en construcción. *Roc Maquina*, 9, 24-27.

Pereira, M.D., Yenes, M., Blanco, J.A., & Peinado, M. (2007). Characterization of serpentinites to define their appropriate use as dimension stone. In R. Prikryl, B.J. Smith, (Ed.), *Building Stone Decay: From Diagnosis to Conservation* (pp. 55-62). London, United Kingdom: Geological Society

Pereira, M.D., Peinado, M., Blanco, J.A., & Yenes, M. (2008). Geochemical characterization of serpentinites at cabo ortegal, northwestern Spain. *Canadian Mineralogist*, 46, 317-327.

Pereira, D. (2012). A report on serpentinites in the context of heritage stone resources. *Episodes*, 35(4), 478-480. https://doi.org/10.18814/epiiugs/2012/v35i4/003.

Pereira, M.D., & Peinado, M. (2012). Serpentinite. *Geology Today*, 28(4), 152-156. https://doi.org/10.1111/j.1365-2451.2012.00844.x.

Pereira, M.D., Blanco, J.A., & Peinado, M. (2013). Study on Serpentinites and the Consequence of the Misuse of Natural Stone in Buildings for Construction. *Journal of Materials in Civil Engineering*, 25(10), 1563–1567. https://doi.org/10.1061/(ASCE)MT.1943-5533.0000689.

Perkins, R.A., Hargesheimer, J., & Fourie, W. (2007). Asbestos release from whole building demolition of buildings with asbestos-containing material. *Journal of Occupational and Environmental Hygiene*, 4, 889-894.

Pierdzig, S. (2019). Regulations Concerning Naturally Occurring Asbestos (NOA) in Germany—Testing Procedures for Asbestos. *Environmental & Engineering Geoscience*, 26 (1), 67–71.

Puga, E., Fanning, M., Díaz de Federico, A., Nieto, J.M., Beccaluva, L., Bianchini, G., et al. (2011). Petrology, geochemistry and U–Pb geochronology of the Betic Ophiolites: Inferences for Pangaea break-up and birth of the westernmost Tethys Ocean. *Lithos*, 124(3-4), 255-272. https://doi.org/10.1016/j.lithos.2011.01.002.

Pugnaloni, A., Giantomassi, F., Lucarini, G., Capella, S., Bloise, A., Di Primio, R., & Belluso, E. (2013). Cytotoxicity induced by exposure to natural and synthetic tremolite asbestos: An in vitro pilot study. *Acta histochemical*, 115, 100–112. DOI:10.1016/j.acthis.2012.04.004

Punturo, R., Cirrincione, R., Pappalardo, G., Mineo, S., Fazio, E., & Bloise, A. (2018a). Preliminary laboratory characterization of serpentinite rocks from Calabria (southern Italy) employed as stone material. *Journal of Mediterranean Earth Science, 10*, 79–87.

Punturo, R., Ricchiuti, C., Mengel, K., Apollaro, C., De Rosa, R., & Bloise, A. (2018b). Serpentinite-derived soils in southern Italy: Potential for hazardous exposure. *Journal of Mediterranean Earth Science, 10*, 51–61.

Punturo, R., Ricchiuti, C., Rizzo, M., & Marrocchino, E. (2019). Mineralogical and Microstructural Features of Namibia Marbles: Insights about Tremolite Related to Natural Asbestos Occurrences. *Fibers*, *7*, 31.

Ross, M., & Nolan R.P., (2003). History of asbestos discovery and use and asbestos-related disease in context with the occurrence of asbestos within ophiolite complexes. *Geological Society of America Special paper*, 373, 447-470.

Sanz de Galdeano, C., & López Garrido, A.C. (2016). The Nevado-Filábride Complex in the western part of Sierra de los Filabres (Betic Internal Zone), structure and lithologic succession. *Boletìn Gològico y Minero*, 127 (4), 823-836. https://doi.org/10.21701/bolgeomin.127.4.005.

Schindelin, J., Arganda-Carreras, I., Frise, E., Kaynig, V., Longair, M., Pietzsch, T., et al. (2012). Fiji: an open-source platform for biological-image analysis. Nature Methods, 9(7), 676–682.

Stroink, G., Blaauw, C., White, C.G., & Leiper, W. (1980). Mössbauer characteristics of UICC standard reference asbestos samples. *Canadian Mineralogist*, 18, 285-290.

Turci, F., Tomatis, M., & Pacella, A. (2017). Surface and bulk properties of mineral fibres relevant to toxicity. In A.F. Gualtieri (Ed.), *Mineral Fibers: Crystal Chemistry, Chemical-Physical Properties, Biological Interaction and Toxicity* (pp. 171-214). London, UK: European Mineralogical Union.

Vignaroli, G., Ballirano, P., Belardi, G., & Rossetti, F. (2014). Asbestos fibre identification vs. evaluation of asbestos hazard in ophiolitic rock mélanges, a case study from the Ligurian Alps (Italy). *Environmental Earth Sciences*, *72*(9), 3679-3698.

Whitney, D., & Evans, B.W., (2010). Abbreviations for names of rock-forming minerals. *American Mineralogist*, 95 (1), 185–187.

WHO, 1997. Determination of Airborne Fibre Number Concentrations; a Recommended Method, by Phase Contrast Optical Microscopy. World Health Organization, Geneva, Switzerland.

Yoon, S., Yeom, K., Kim, Y., Park, B., Park, J., Kim, H., Jeong, H., & Roh, Y. (2019). Management of Naturally Occurring Asbestos Area in Republic of Korea. *Environmental & Engineering Geoscience*, 26 (1), 79–87.

Figure Captions

Fig. 1 Geological setting and location of the quarries: 1 = Barranco de San Juan, 2 = Nigüelas, 3 = Virgen del Rosario, 4 = La Carrasca (Modified after Martin-Algarra et al. 2004)

Fig. 2 Distant view of the quarries: **a** Barranco the San Juan, **b** Nigüelas, **c** Virgen de Rosario, **d** La Carrasca

Fig. 3 Pictures taken at the quarry of: **a** Barranco the San Juan, detail of a tremolite vein (between the dashed red lines) cross-cutting serpentinite, **b** Nigüelas, outcrop with white asbestos tremolite (Tr), **c** Virgen de Rosario, network of veins developed inside the massive serpentinite, indicated by the black arrows, **d** La Carrasca, appearence of green serpentinite cut by veins filled with tremolite, indicated by the black arrow

Fig. 4 Comparison between differential scanning calorimetry (DSC) curves of the studied samples, the insets show magnification of DSC curves with arbitrary unit of the heat flow

Fig. 5 Comparison between differential scanning calorimetry (DTG) curves of the studied samples, the insets show magnification of DTG curves

Fig. 6 Scanning electron micrographs: **a** chrysotile bundles (sample VG1), **b** chrysotile bundles (sample CA1), **c** chrysotile bundles (sample VG2), **d** zoom of **b** showing chrysotile separable fibres with and the relative energy-dispersive spectrometry (EDS) point analysis

Fig. 7 a Scanning electron micrograph of tremolite, **a** fibrous and prismatic habit (NG sample). **b** fibrous tremolite (CA1 sample), the insert shows fibre flexibility. **c** fibrous tremolite (CA1 sample), the inserts indicated by the orange and blue arrows show longitudinal splitting of the fibre. **d** fibrous tremolite over prismatic tremolite (NG sample) the insert indicated by green arrow shows both flexibility and easiness of the fibre to split

Fig. 8 Amphibole diagram classification (after Leake et al. 1997)

Fig. 9 Left column: Volume renderings of extracted VOIs from samples CA1 (**a**, **b** - 5.24 mm^3) and CA2 (**c**, **d** - 5,67mm^3). Right column: corresponding segmented veins/pore phase. The white arrows indicate the veins/voids

Figure 1

Click here to access/download;Figure;Fig. 1.tif

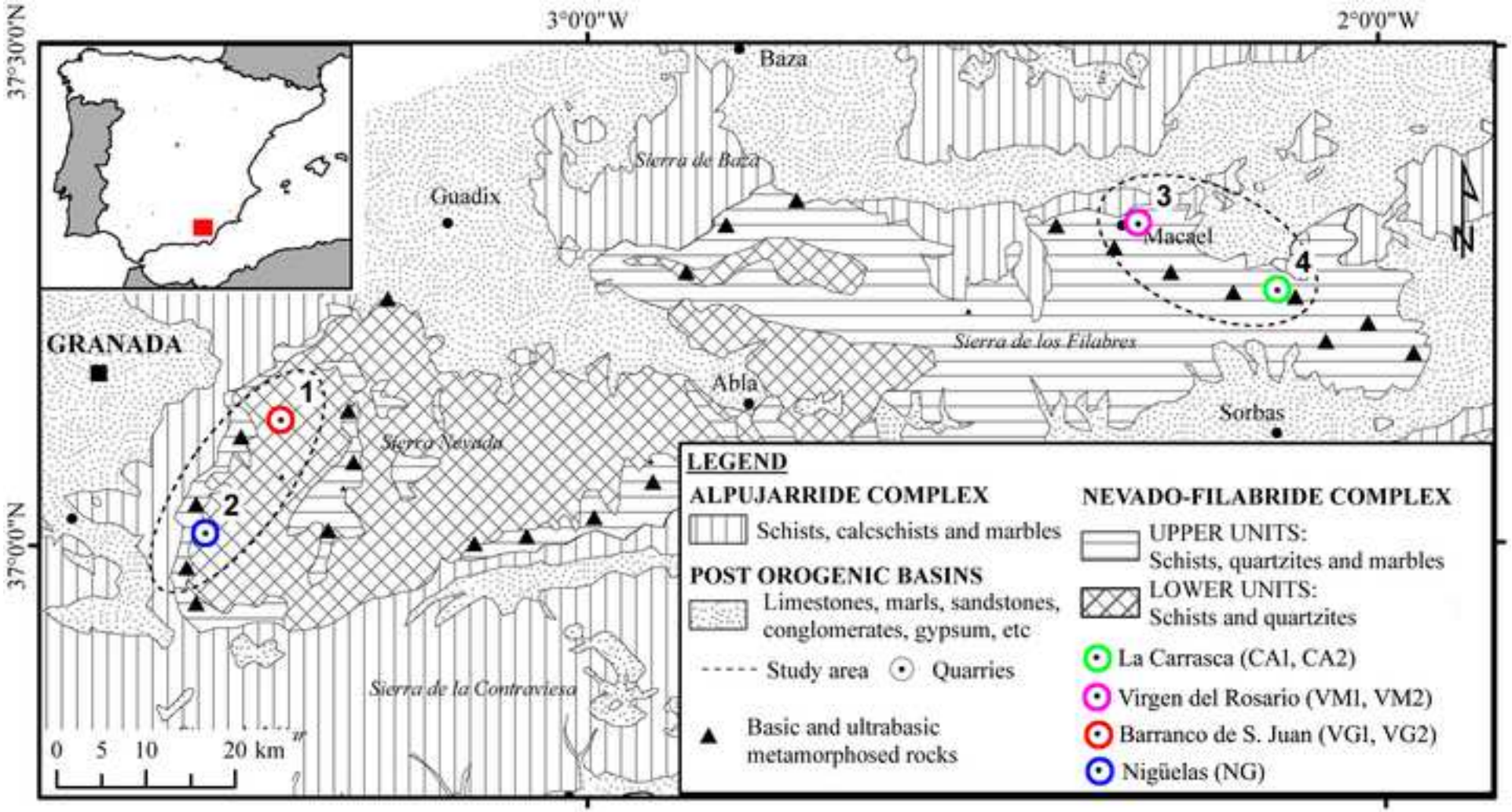

Figure 2

Click here to access/download;Figure;FIg. 2.jpg

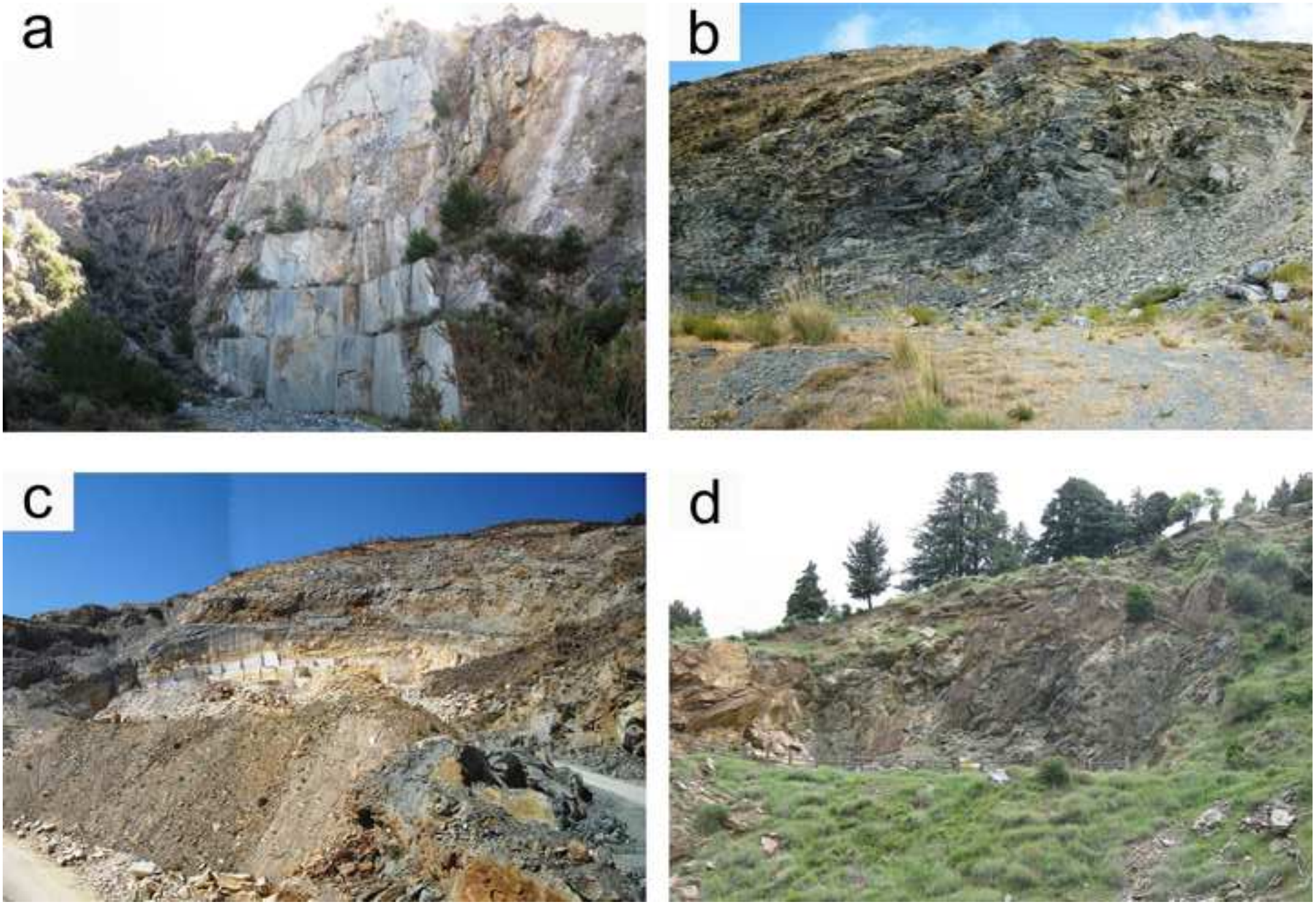

Figure 3

Click here to access/download;Figure;Fig. 3.jpg

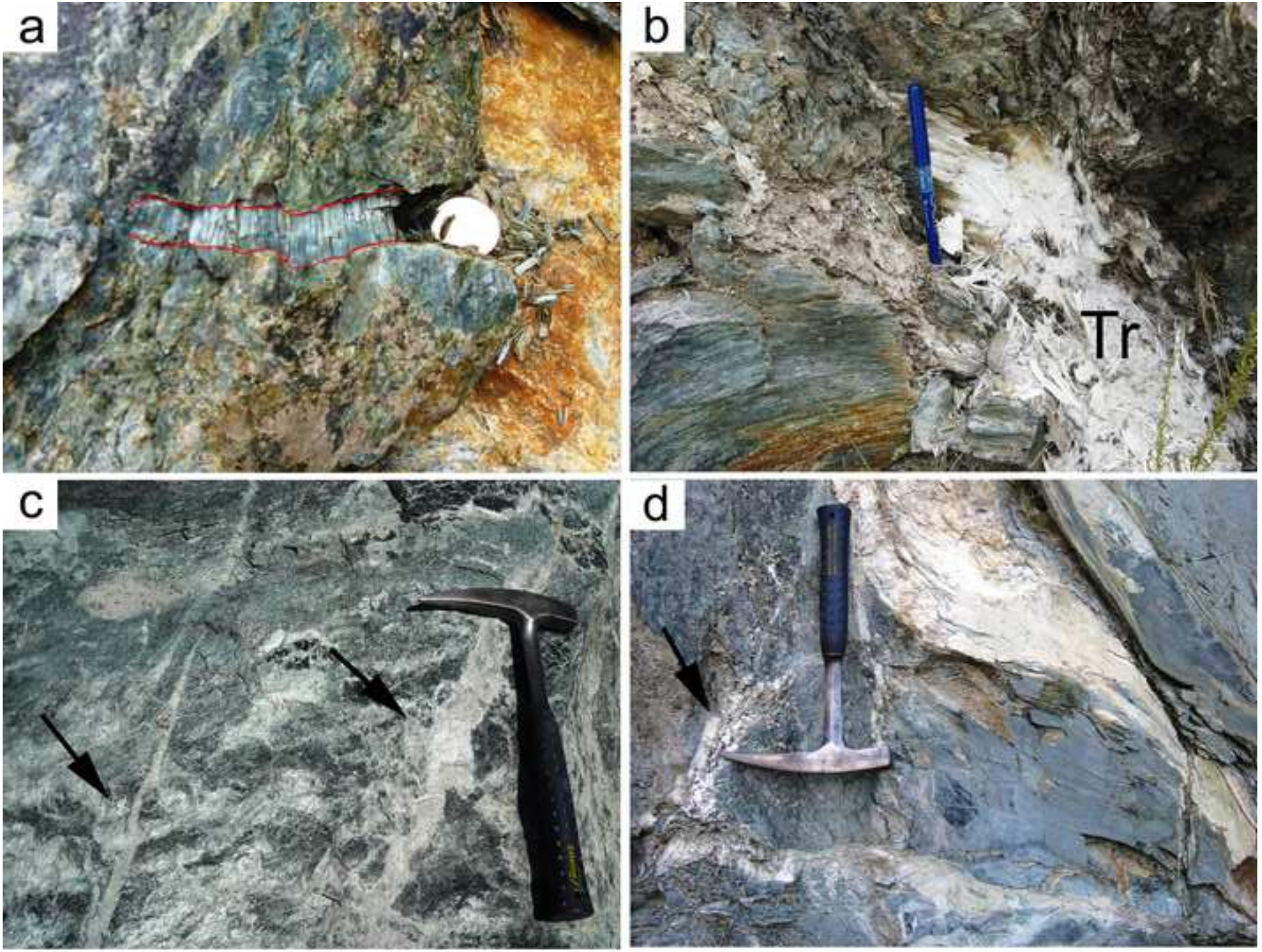

Figure 4

Click here to access/download;Figure;Fig. 4.jpg

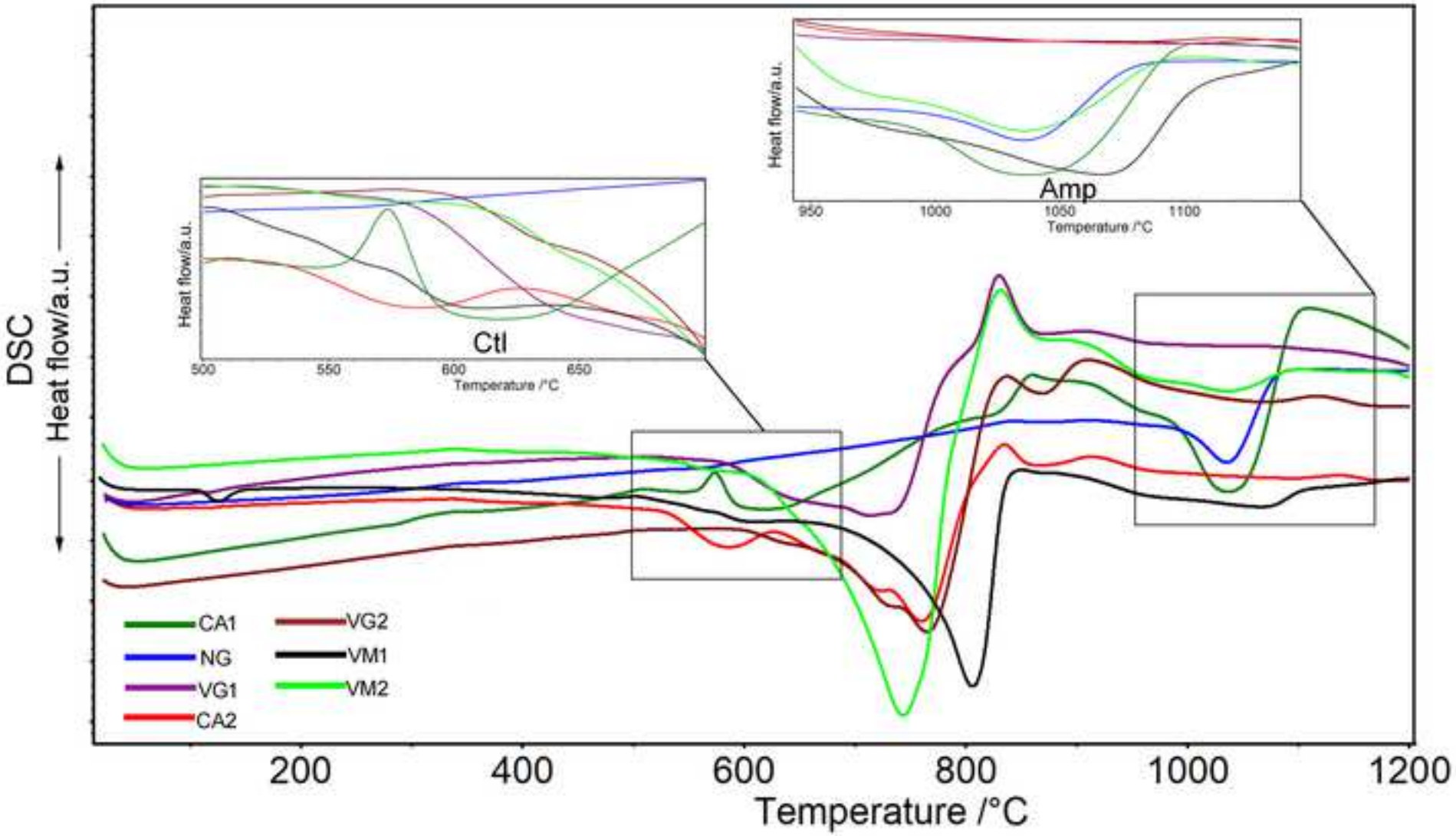

Figure 5

Click here to access/download;Figure;Fig. 5.jpg

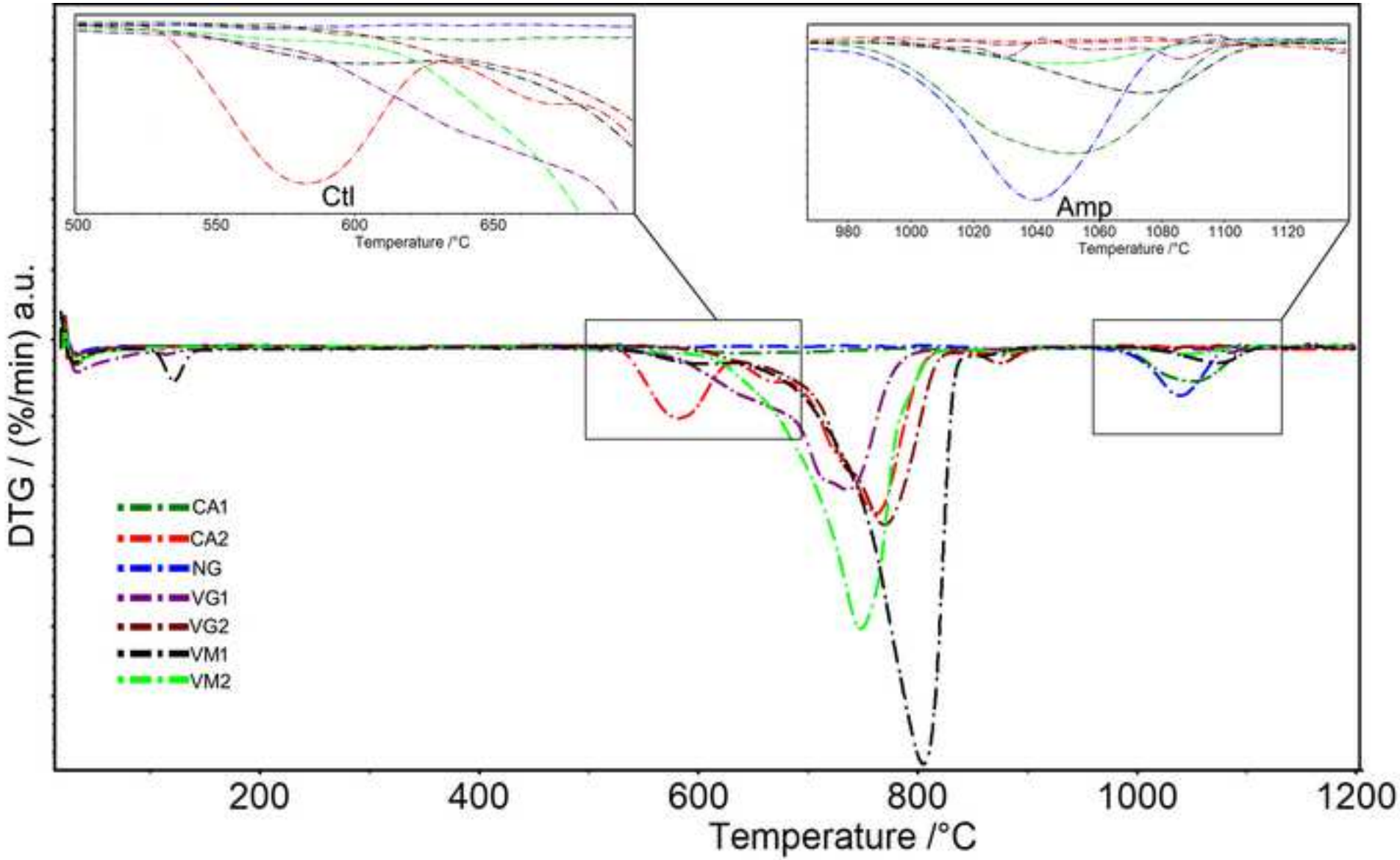

Figure 6

Click here to access/download;Figure;Fig. 6.jpg

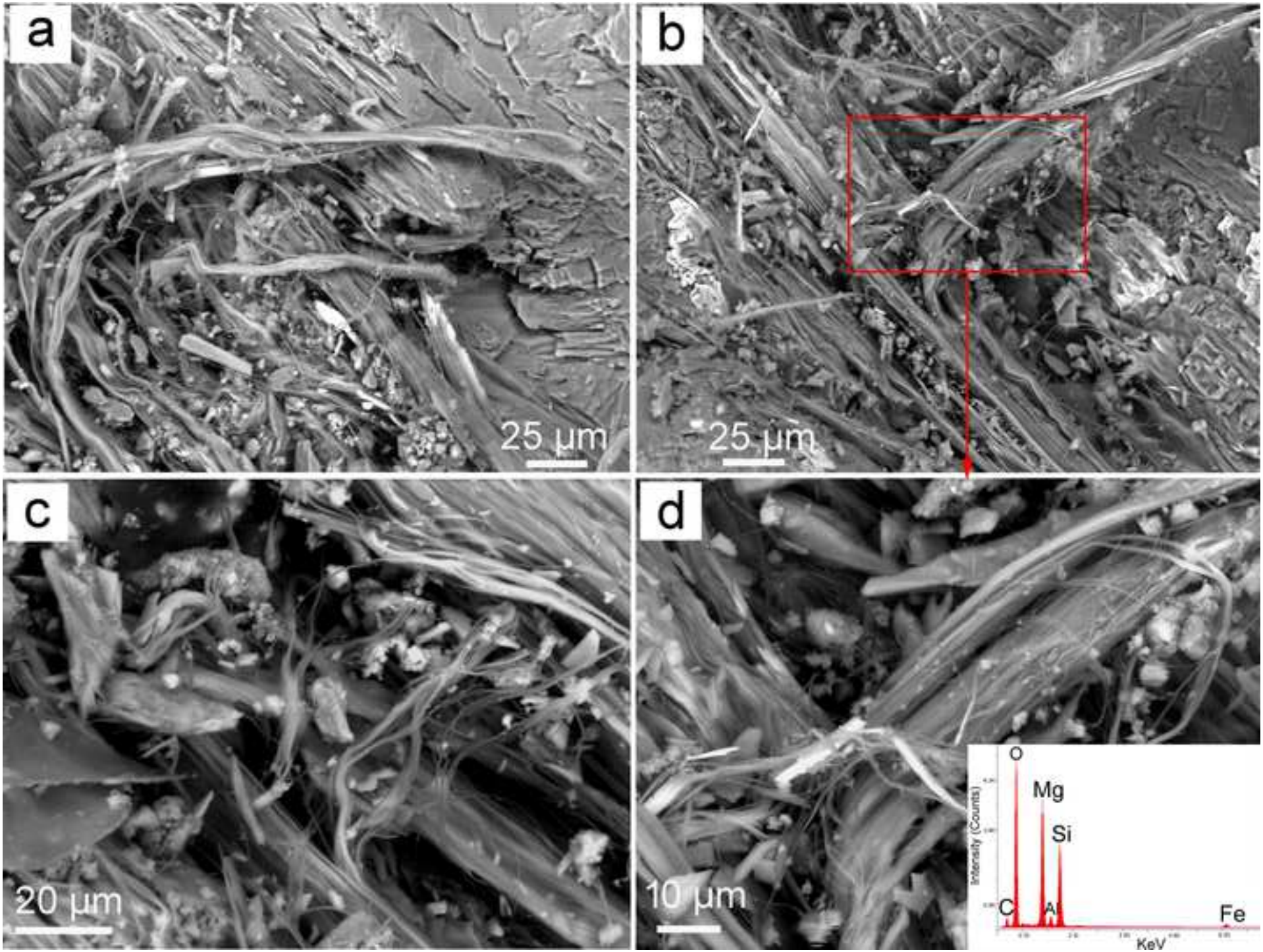

Figure 7

Click here to access/download;Figure;Fig. 7.jpg

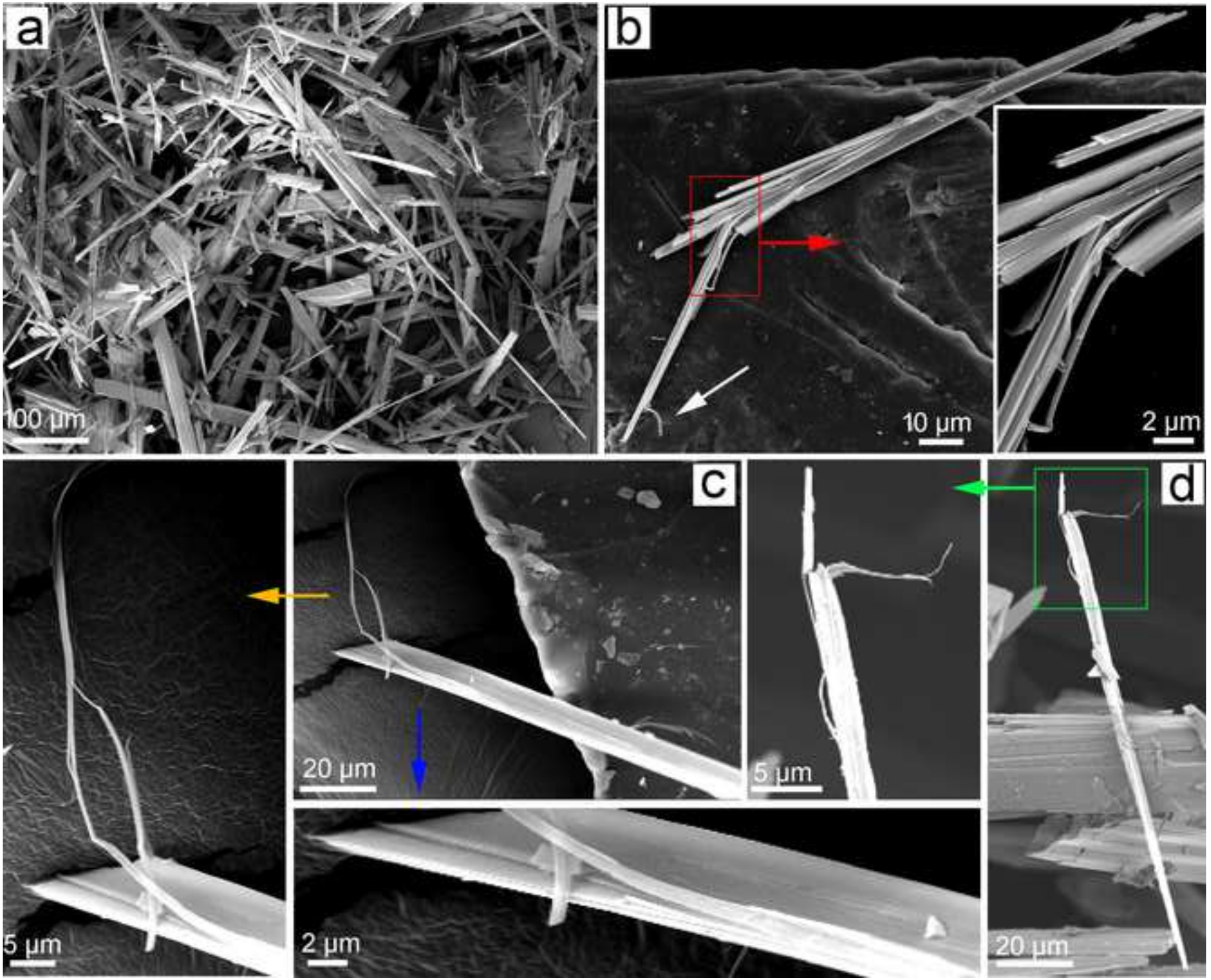

Figure 8

Click here to access/download;Figure;Fig. 8.tif

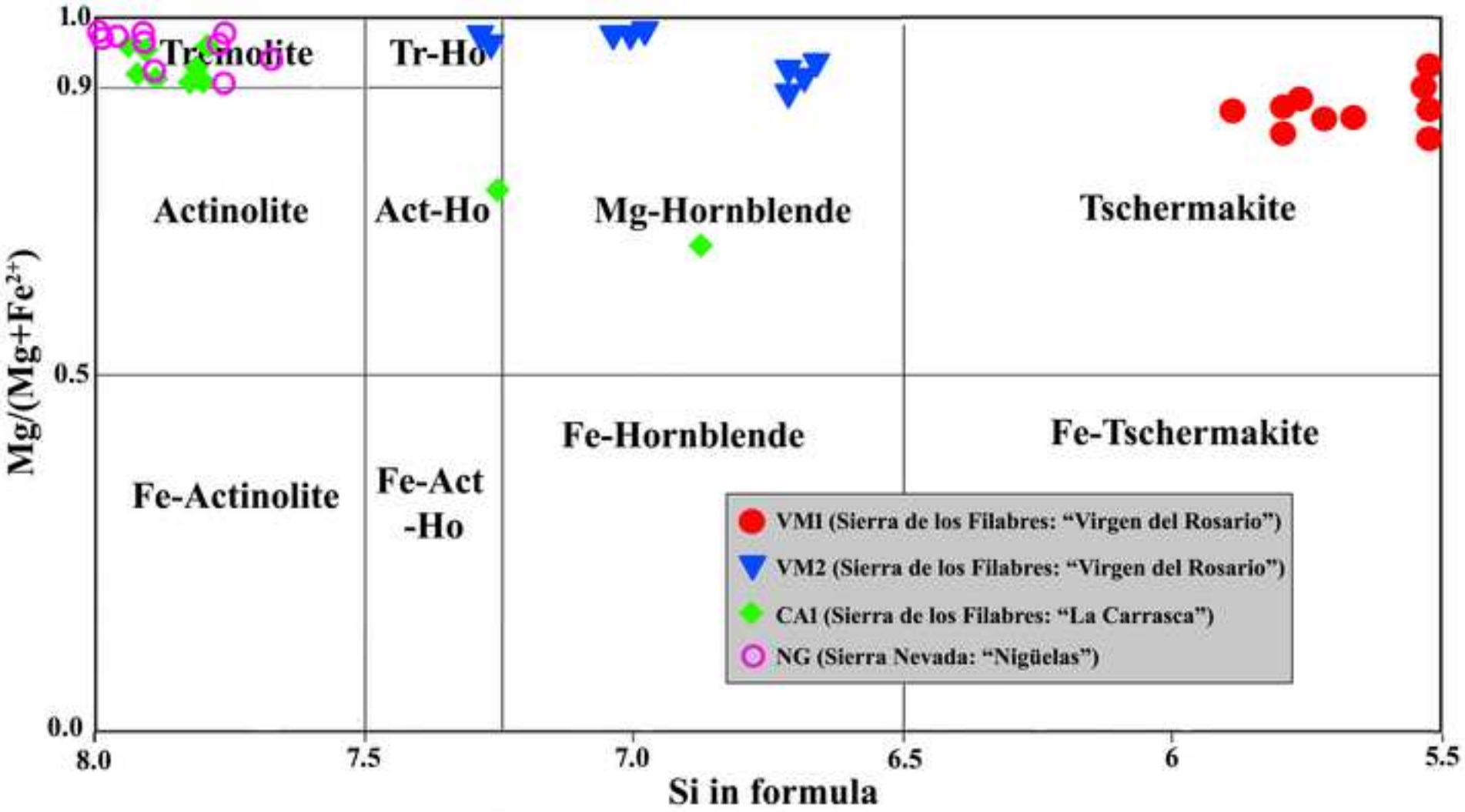

Figure 9

Click here to access/download;Figure;Fig. 9.tif

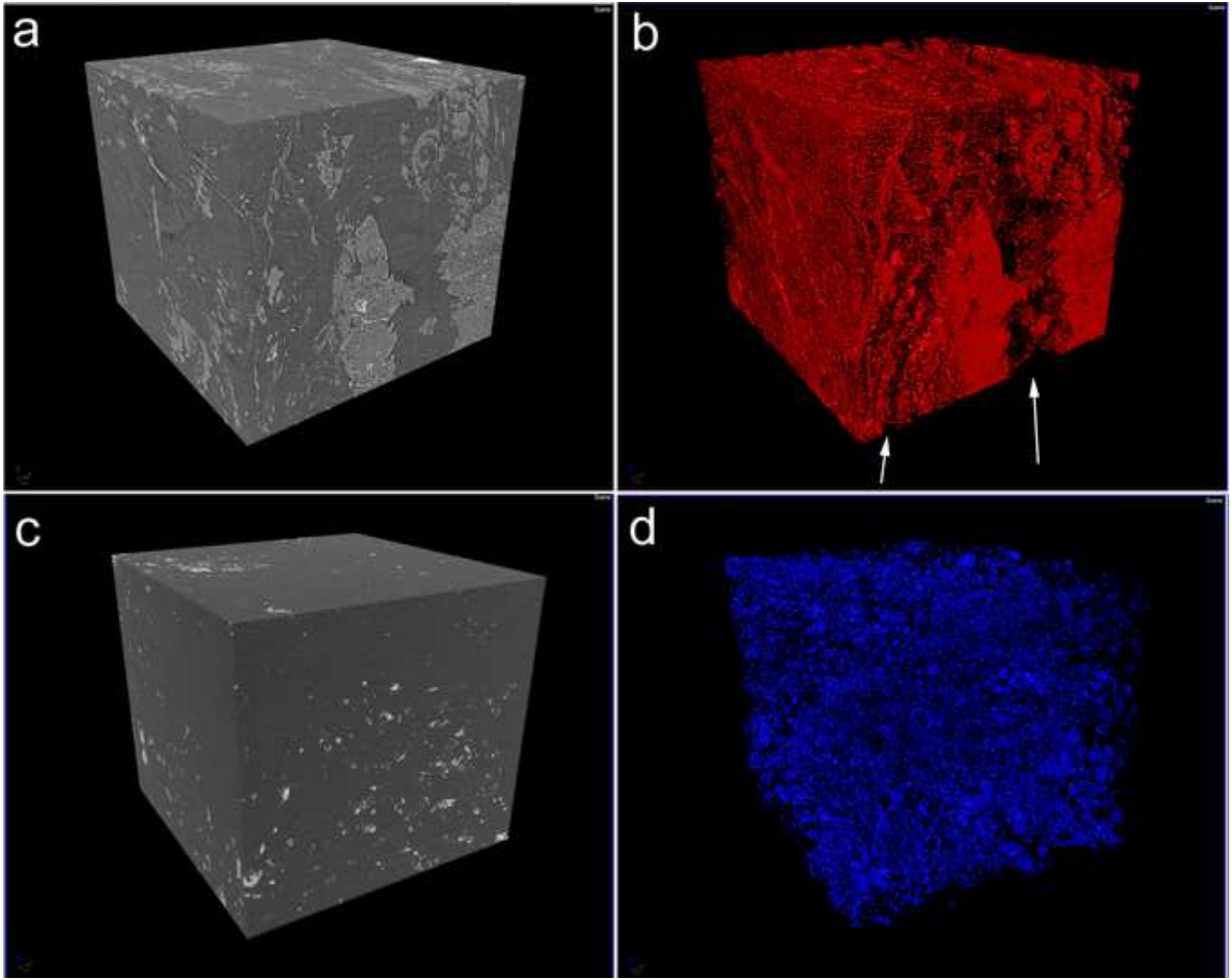

Table 1 Click here to access/download;Table;Table 1.docx

Sample	Mesoscopic description	Locality	Quarry	Phases detected
VG1	Massive	Granada	Barranco de San Juan	Liz>PS>Ctl
VG2	Massive	Granada	Barranco de San Juan	Ant>Cal>Liz>Ctl>Mag
NG	Fibrous	Granada	Nigüelas	Tr>>Cal>Chl>Ant>PS>Mag
VM1	Massive	Macael	Virgen del Rosario	Dol>Ts>Chl>Clay>Qtz
VM2	Evident fibrous veins	Macael	Virgen del Rosario	Liz>>Hbl-Tr>Chl>Ctl>Dol>Ant>Mag
CA1	Fibrous	Almeria	La Carrasca	Tr>>Ctl>Chl>Qtz>Mag>Dol
CA2	Massive	Almeria	La Carrasca	Ant>>Chl>Liz>Cal>PS>Mag>Clay

Table 1 Semi-quantitative mineralogical composition of samples in order of decreasing relative abundance, detected by XRPD, DSC/DTG and EDS/SEM. Ctl = chrysotile, Liz = lizardite, Ant = antigorite, PS = polygonal serpentine, Tr = tremolite, Hbl = hornblende, Ts = tschermakite, Mag = Magnetite, Dol = dolomite, Cal = calcite, Qz = quartz, Chl = Chlorite, Clay= Clay minerals. Mineral symbols after Whitney and Evans (2010)

DSC (T °C)							
Phases	**VG1**	**VG2**	**NG**	**VM1**	**VM2**	**CA1**	**CA2**
Clay				121 endo			125 endo
Mag		340 exo	349 exo		338 exo	339 exo	373 exo
Chl			563 endo	562 endo	574 endo w	543 endo	595 endo
Qz				502 exo		573 exo s	
Ctl	640 endo	622 endo w			644 endo vw	620 endo	
PS	717 endo						
Liz	735 endo w	720 endo			744 endo s		722 endo
Atg		770 endo					760 endo
Fo*	828 exo	823 exo			878 endo w	858 exo	
Dol/cal		875 endo	880 endo	806 endo	800 sh	860 endo	870 endo
Tr/Hbl/ Ts			1039 endo	1070 endo	1043 endo	1053 endo	
Px*			1135 v w	1143 w exo	1110 exo	1103 exo	
DTG (T °C)							
Clay				122 endo			123 endo
Chl			564 endo	560 endo	565 endo	544 endo	585 endo s
Ctl	638 endo	636 endo w			640 sh	622 endo	
PS	717 endo		699 endo vw				670 endo
Liz	735 endo w	732 endo					722 endo
Atg		770 endo	781 endo vw		744 endo		760 endo s
Dol				806, 863 endo s	805, 860 sh	831, 862 endo	
Cal		876 endo	880 endo				878 endo
Tr/Hbl/Ts			1039 endo s	1074 endo	1045 endo w	1053 endo	

Table 2 Peak temperature values in DSC and DTG curves. w = weak, s = strong, sh = shoulder, endo = endothermic, exo = exothermic, Atg = antigorite, Lz = lizardite, Ctl = chrysotile, PS = polygonal serpentine, Chl = chlorite, Tr = tremolite, Hbl= hornblende, Ts = tschermakite, Fo = forsterite, Px = pyroxene, Dol = dolomite, Cal = calcite, Qz= quartz, Mag = magnetite, Clay m = clay minerals. *New phases formed after the breakdown. Mineral symbols after Whitney and Evans (2010)

Click here to access/download;Table;Table 3.docx

Samples		VG1			VG2			VM2			CA1	
Oxide wt.%	Ctl	Ctl	Ctl	Ctl	Ctl	Ctl	Ctl	Ctl	Ctl	Ctl	Ctl	Ctl
SiO_2	44.61	44.63	44.96	44.01	42.14	43.83	47.34	43.17	44.5	44.97	42.15	44.66
Al_2O_3	2.49	4.71	3.17	4.97	4.10	4.28	2.83	4.69	2.51	3.15	4.00	2.46
MgO	44.58	46.85	46.27	45.48	42.12	42.66	44.32	44.29	44.47	46.29	42.13	44.63
FeO	4.40	3.81	2.68	3.76	7.34	5.55	5.51	4.80	4.60	2.67	7.36	4.33
CaO	2.26	0.00	2.92	1.78	2.05	1.98	0.00	1.65	2.24	2.92	2.09	2.23
Cr_2O_3	0.28	0.00	0.00	0.00	0.00	0.00	0.00	0.00	0.29	0.00	0.00	0.29
NiO	1.38	0.00	0.00	0.00	2.25	1.70	0.00	1.40	1.39	0.00	2.27	1.40
CATIONS calculated on the basis of 7 oxigens												
Si	1.86	1.83	1.85	1.82	1.79	1.84	1.95	1.80	1.86	1.85	1.80	1.86
Al	0.12	0.23	0.15	0.24	0.21	0.21	0.14	0.23	0.12	0.15	0.20	0.12
Mg	2.77	2.87	2.84	2.80	2.67	2.67	2.72	2.76	2.77	2.84	2.67	2.78
Fe^{2+}	0.15	0.13	0.09	0.13	0.26	0.20	0.19	0.17	0.16	0.09	0.26	0.15
Ca	0.00	0.00	0.13	0.08	0.09	0.09	0.00	0.07	0.10	0.13	0.10	0.10
Cr	0.01	0.00	0.00	0.00	0.00	0.00	0.00	0.00	0.01	0.00	0.00	0.01
Ni	0.05	0.00	0.00	0.00	0.08	0.06	0.00	0.05	0.05	0.00	0.08	0.05

Table 3 Three representative EDS/SEM analyses point of chrysotile fibres from four samples, normalized oxide weight percent and cation number calculated on the basis of seven oxygens

Click here to access/download;Table;Table 4.docx

Samples	CA1_Tremolite								NG_Tremolite									
MgO	25.55	22.32	25.96	25.69	24.65	24.03	23.84	24.25	23.84	24.99	24.92	23.89	27.01	25.84	25.62	22.88	22.53	26.57
Al_2O_3	1.22	2.26	0.29	0.25	1.00	0.32	0.01	2.20	0.74	1.06	1.30	0.54	2.48	2.30	2.08	2.02	2.02	0.48
SiO_2	60.00	58.79	60.68	59.00	60.32	58.82	59.24	60.19	60.00	60.02	60.09	60.99	59.08	58.02	58.62	59.79	58.45	61.08
CaO	10.98	11.76	11.44	11.9	9.83	12.01	11.93	11.53	13.48	11.62	12.06	12.75	9.91	11.02	12.03	11.76	12.76	9.99
Cr_2O_3	0.00	0.56	0.00	0.00	0.00	0.00	0.00	0.00	0.00	0.00	0.00	0.00	0.00	0.00	0.00	0.00	0.00	0.00
FeO	2.25	3.87	1.63	3.16	4.20	4.82	4.98	1.83	1.93	2.31	1.63	1.83	1.52	2.82	1.65	3.55	4.24	1.88
Na_2O	0.00	0.44	0.00	0.00	0.00	0.00	0.00	0.00	0.00	0.00	0.00	0.00	0.00	0.00	0.00	0.00	0.00	0.00
Mg	5.01	4.42	5.09	5.08	4.83	5.08	4.72	4.75	4.71	4.91	4.89	4.69	5.28	5.09	5.05	4.50	4.46	5.15
Al^{3+}	0.11	0.20	0.02	0.04	0.07	0.05	0.002	0.09	0.04	0.09	0.08	0.01	0.25	0.33	0.25	0.11	0.23	0.003
Si	7.90	7.80	7.98	7.82	7.93	7.82	7.87	7.91	7.96	7.91	7.92	8.04	7.75	7.67	7.75	7.89	7.76	7.95
Ca	1.55	1.67	1.61	1.70	1.39	1.71	1.70	1.62	1.92	1.64	1.70	1.8	1.39	1.56	1.70	1.66	1.82	1.40
Cr	0.00	0.06	0.00	0.00	0.00	0.00	0.00	0.00	0.00	0.00	0.00	0.00	0.00	0.00	0.00	0.00	0.00	0.00
Fe^{2+}	0.25	0.43	0.18	0.35	0.46	0.54	0.50	0.20	0.14	0.26	0.18	0.20	0.17	0.31	0.18	0.39	0.47	0.21
Na	0.00	0.11	0.00	0.00	0.00	0.00	0.00	0.00	0.00	0.00	0.00	0.00	0.00	0.00	0.00	0.00	0.00	0.00

Table 4 Representative EDS/SEM analyses of tremolite fibres (CA1 and NG samples), normalized oxide weight percent and cation number calculated on the basis of 23 oxygens

Cover letter

Click here to view linked References

Click here to access/download;attachment to manuscript;Cover_letter_NOAS.doc

UNIVERSITÀ DELLA CALABRIA

DiBEST
Dipartimento di Biologia, Ecologia e Scienze della Terra

University of Calabria,
Department of Biology, Ecology and Earth Sciences,
C15-b, 87036 Arcavacata di Rende, CS, Italy
Professor **Andrea Bloise**
e-mail: andrea.bloise@unical.it

Rende, May 10, 2020

Dear Editor,

The manuscript entitled "***Naturally occurring asbestos in quarries: southern Spain as a case study***" has been carefully checked and approved by all authors **(A. Bloise, C. Ricchiuti, R. Navarro, R. Punturo, G. Lanzafame, D. Pereira)**. The work has not been published and is not being considered for publication elsewhere in whole or in part in any language. Furthermore, there is no other work in preparation, submitted, in press or published from our/my laboratory which overlaps the contents of this paper.

It is universally recognised that natural occurring asbestos (NOA) can adversely affect human health and it is therefore essential to detect asbestos minerals from both a scientific and legislative perspective, especially for the administrative agencies whose main responsabilities are to safeguard public health and implement construction and safeguard policies (e. g., civil constructions, building stones, road yards and quarry excavations).

The manuscript is focused on the detection of asbestos in serpentinitic rock, in order to understand their possible contribution to the health problems. At this purpose, seven serpentinite rock samples have been collected from quarries located in Sierra Nevada and Sierra de los Filabres (Southeastern Spain) and characterized in detail, cross the data obtained from different analytical techniques: X-ray powder diffractometry (XRPD), scanning electron microscopy combined with energy-dispersive spectrometry (SEM/EDS), differential scanning calorimetry (DSC), derivativethermogravimetry (DTG) and X-ray synchrotron microtomography (SR-µCT).

In our opinion, this approach is the best way to identify the asbestos phases present in the serpentinitic rocks as excluding the occurrence of errors derived from the inability to distinguish serpentine polymorphs using only XRPD and/or SEM/EDS. Moreover, SR-µCT has proven to be a complementary technique to other conventional ones which may prove useful in the event of environmental pollution by asbestos. The role of toxic element concerning the asbestos-related health effects, was also discussed. The present study revealed that serpentinites cropping out from quarries located in Sierra Nevada and Sierra de los Filabres (Southeastern Spain) could act as a perennial source of contamination for the surrounding environment. To our knowledge this is the first paper that deals with NOA in Spain.

I will act as corresponding author.

Best regards

Prof. Andrea Bloise

Declaration

Click here to view linked References

Click here to access/download;attachment to manuscript;Declarations.doc

UNIVERSITÀ DELLA CALABRIA

DiBEST
Dipartimento di Biologia, Ecologia e Scienze della Terra

University of Calabria,
Department of Biology, Ecology and Earth Sciences,
C15-b, 87036 Arcavacata di Rende, CS, Italy
Professor **Andrea Bloise**
e-mail: andrea.bloise@unical.it

Rende, May 09, 2020

Dear Editor
on behalf of all the co-authors I declare

Declarations

Funding
No funding was received.

Conflicts of interest
The authors declare that that there is no conflict of interest

Availability of data and material
All the raw data and material used for this research is available at the University of Calabria and University of Catania for request.

Best Regards

Prof. Andrea Bloise